Nonlinear Nanodevices Using Magnetic Flux Quanta

S. Ooi,[1] Sergey Savel'ev,[2,3] M. B. Gaifullin,[1,3] T. Mochiku,[1] K. Hirata,[1] and Franco Nori[2,4]

[1]*National Institute for Materials Science, Sengen 1-2-1, Tsukuba, Ibaraki 305-0047, Japan*

[2]*Frontier Research System, The Institute of Physical and Chemical Research (RIKEN), Wako-shi, Saitama, 351-0198, Japan*

[3]*Department of Physics, Loughborough University, Loughborough LE11 3TU, United Kingdom*

[4]*Department of Physics and MCTP, The University of Michigan, Ann Arbor, Michigan 48109-1040, USA*

(Received 21 June 2007; published 16 November 2007)

All devices realized so far that control the motion of magnetic flux quanta employ either samples with nanofabricated spatially-asymmetric potentials (which strongly limit controllability), or pristine superconductors rectifying with low-efficiency time-asymmetric oscillations of an external magnetic field. Using layered $Bi_2Sr_2CaCu_2O_{8+\delta}$ materials, here we fabricate and simulate two efficient nonlinear superconducting devices with *no* spatial asymmetry. These devices can rectify with high-efficiency a two-harmonic external current dragging vortices in target directions by changing either the relative phase or the frequency ratio of the two harmonics.

DOI: 10.1103/PhysRevLett.99.207003 PACS numbers: 85.25.−j, 74.25.Qt

The dynamics of magnetic flux quanta in superconductors (i.e., vortices) share similarities [1] with quanta of electrical charge (i.e., electrons) in solids. Exploring novel ways [2–15] to control the motion of vortices could be useful for fluxtronic devices, i.e., new ''electronic'' devices employing vortices instead of electrons. These vortex devices [2–15] could be used, e.g., to remove unwanted flux from either SQUIDs or qubits, to sculpt magnetic profiles on submicron scales, or to control the spin polarization in spintronic systems.

Recently, vortex ratchets have been built using spatially-asymmetric pinning arrays in order to control vortex motion. Vortex pumps and diodes employing samples with spatial asymmetry to rectify ac drives have been recently proposed [3–6] and realized [7–15]. However, spatially-asymmetric potentials are fixed and cannot be changed after fabrication. Thus, even though these devices sometimes allow one to reverse (e.g., [8,14,15]) the net vortex motion by changing the applied magnetic field, their controllability is limited. For instance, there is no way to change the direction of the vortex motion for fixed vortex density and current.

These problems can be solved by using *nonlinear* flux quanta devices (e.g., Ref. [16,17]) and applying a time-asymmetric zero-averaged ac current or magnetic field. Because of the absence of fixed spatial asymmetry, the vortex motion is fully controlled by changing the shape of the input signal, which is very easy to manipulate. The first attempts to realize this approach [18,19] were done for samples with no pinning potential. Unfortunately, this often produces a weak nonlinearity, resulting in a small efficiency of these nonlinear rectifiers.

Here, we experimentally prove and numerically show that combining a *spatially-symmetric* nanofabricated potential substrate with a drive having *two harmonics* [20] allows one to conveniently manipulate vortex motion with high efficiency, e.g., pushing magnetic quanta either to the right or to the left by changing either the *relative phase* of the harmonics in the drive or their *frequency ratio*. Moreover, the nonlinearity responsible for this rectification can be controlled by an applied magnetic field.

Using entirely different types of samples, we also experimentally show that nonlinear rectifiers of Josephson vortex (JV) oscillations, which are induced by a two-harmonic out-of-plane electrical current, become very efficient when increasing a c-axis magnetic field $H_\perp$. The physical origin of this enhancement of the rectification effect is related to the increase of the density of c-axis-aligned magnetic flux quanta [i.e., pancake vortices (PVs)] which pin [21] the JVs located between planes. This mutual interaction between JVs and PVs allows controlling the motion of JVs, e.g., by varying the frequency ratio of the two harmonic drives.

Sample fabrication and experimental setup.—High-quality $Bi_2Sr_2CaCu_2O_{8+\delta}$ single crystals were grown by the travelling-solvent floating-zone technique [22]. These crystals were used to fabricate two very different types of nonlinear nanodevices (Figs. 1 and 2) to manipulate the motion of either PVs or JVs.

When making the structure shown in the micrograph in Fig. 1(b), thin $Bi_2Sr_2CaCu_2O_{8+\delta}$ single-crystal films (thickness between 100 and 300 nm) for the four-terminal measurements [Fig. 1(b), inset] were fabricated using a photolithographic and Ar-ion milling processes. Holes patterned as a triangular lattice, to efficiently pin vortices, were milled by a focused ion beam (FIB). The diameter of each hole was about 300 nm, while the interhole distance a_0 was 1 μm. The superconducting transition temperature T_c was 87.8 K. The magnetoresistance of the sample showed clear matching peaks when the number of vortices was a multiple of the number of pinning centers, i.e., for magnetic fields $H_n^{\rm match} = 2n\Phi_0/\sqrt{3}a_0^2$, where n is an integer and Φ_0 is the flux quantum. This indicates that the fabricated pinning potential efficiently pins pancake vortices.

Figure 2 shows results from a different type of device (from the one discussed above) controlling the motion of

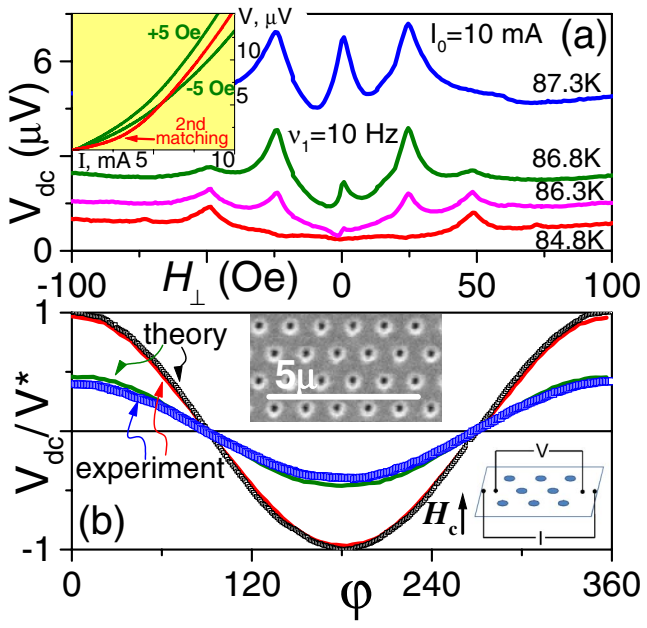

FIG. 1 (color online). *Out-of-plane flux quanta rectifier.*—Panel (a): Rectified dc voltage (which is proportional to the drift vortex velocity) as a function of the out-of-plane magnetic field $H_\perp$ at different temperatures. Inset in Panel (a): Nonlinear voltage-current characteristics of the device shown in panel (a) at the second matching field H_2^{match} (red line), and at two other fields shifted ±5 Oe with respect to H_2^{match}. Micrograph in (b): Scanning ion microscopy (SIM) image of a nanofabricated $Bi_2Sr_2CaCu_2O_{8+\delta}$ single-crystal film which has a triangular lattice of holes, which were milled by FIB. The holes have a diameter of about 300 nm and are separated by $a_0 = 1$ μm. Holes trap out-of-plane flux quanta resulting in the very nonlinear vortex dynamics needed for nonlinear rectifiers. Panel (b): Measured rectified dc voltage V_{dc} (red symbols for H_1^{match} and blue symbols for H_2^{match}, both pointed by arrows labeled "experiment") versus relative phase φ between the two harmonics of the driving current $I_{\text{drive}}(\nu_1, \nu_2 = 2\nu_1, \varphi)$. The output dc voltage V_{dc} is normalized by its value $V^* = V_{dc}(\varphi = 0, H_1^{\text{math}})$ at zero phase shift $\varphi = 0$ between the harmonics and for the first matching field, H_1^{match} (i.e., when the number of vortices coincides with the number of holes). The frequency of the second harmonic is chosen here to be twice the frequency of the first harmonic ($\nu_2 = 2\nu_1 = 20$ Hz); the amplitude of each harmonic is $I_0 = 10$ mA, and the temperature 86.8 K. Simulated dc voltages are shown by black symbols for H_1^{match} and by the green line for H_2^{match}, both pointed by arrows labeled "theory." Normalized simulation parameters are $\nu_1 = 0.01$, $r^{(p)} = 0.2$, $\max(|f_L|) = 0.2$, $\max(|f_{pv}|) = 0.3$. Note that by changing φ we can: (i) easily tune the output dc voltage from *negative* $V_{dc}(\varphi = \pi)$ to *positive* $V_{dc}(\varphi = 0)$ values and (ii) obtain a very smooth and predictable dependence for $V_{dc}(\varphi)$. Note that the $V_{dc}(\varphi)$ dependence is similar to the $I(\varphi)$ behavior of a Josephson current between two superconductors as a function of the *phase difference* of the order parameter. Bottom inset in (b): geometry of the problem.

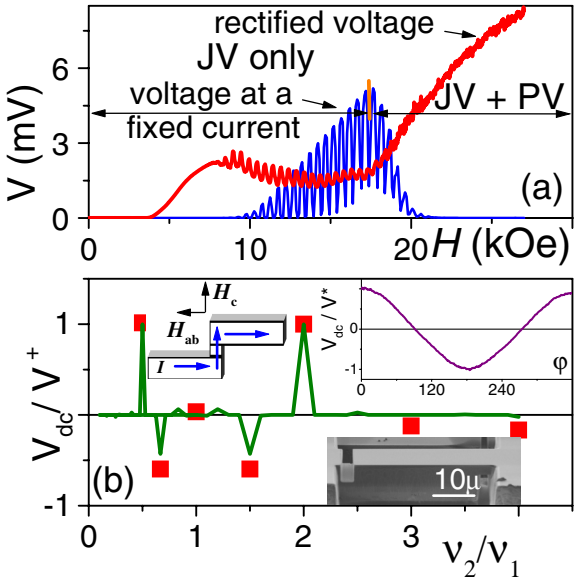

FIG. 2 (color online). *In-plane flux quanta rectifier.*—Panel (a): The blue curve (also pointed by arrow labeled "voltage at a fixed current") shows the flux-flow voltage, measured at a fixed time-independent current of 100 μA, versus an externally applied magnetic field H, which is almost parallel to the CuO_2 layers ($H_\perp \ll H_\parallel$). When increasing the field H, two regimes are clearly distinguished: (1) the "JV only" regime corresponds to the absence of out-of-plane magnetic flux quanta—only JVs are in the system; (2) the "JV + PV" regime, when $H_\perp$ ($\propto H$) is strong enough to create PVs, which act as pinning centers (traps) for JVs—resulting in strongly nonlinear dynamics. The rectified dc voltage (red curve, also pointed by arrow labeled "rectified voltage"), measured when a two-harmonic ac current, $I_{\text{drive}}(\nu_1 = 100$ Hz, $\nu_2 = 2\nu_1, \varphi = 0)$, with amplitude $I_0 = 1$ mA was applied, is low for the weakly nonlinear "JV only" regime, and strongly enhanced in the "JV + PV" regime. Micrograph in (b): SIM image of the fabricated $Bi_2Sr_2CaCu_2O_{8+\delta}$ single-crystal bar for the measurements of Josephson-vortex flow. The device is shaped as a narrow bridge joining large parts of the superconducting bar. The $14.8 \times 24.5 \times 0.6$ μm^3 bridge was fabricated by FIB. Panel (b): Red squares are the measured rectified dc voltage $V_{dc}(\nu_2, \nu_1)$, normalized by $V^+ = V_{dc}(\nu_1, \nu_2 = 2\nu_1)$, versus ν_2, for a fixed $\nu_1 = 100$ Hz when the two-harmonic driving current $I_{\text{drive}}(\nu_1, \nu_2, \varphi = 0)$, with amplitude $I_0 = 1$ mA, is applied. The green line with sharp peaks corresponds to a simulation of $V_{dc}(\nu_2, \nu_1)/V^+$ versus ν_2 using the following normalized parameters $\lambda_c = 2$, $\lambda_{PJ} = 0.5$, $f_{JJ}^0 = 0.5$, $f_{PJ} = 0.5$, $\max(|f_L|) = 3$, $\eta_P/\eta_J = 5$, $\nu_1 = 0.01$. All the measured peaks of the rectified voltage are perfectly reproduced in our simulations. Right inset in panel (b): Experimental $V_{dc}(\nu_2 = 2\nu_1, \nu_1 = 100$ Hz), normalized by $V^* = V_{dc}(\varphi = 0)$, versus relative phase φ between the two harmonics. The $V_{dc}(\varphi)$ Josephson-type dependence shown is very similar to the one [Fig. 1(b)] obtained for our out-of-plane quanta rectifier. The temperature was 10 K for all measurements. Left inset in (b): geometry of the problem.

the JVs. This device was fabricated in the central part of a crystal bar which was milled using an FIB to form a bridge [23]. When manipulating JVs, we use a split magnet to vary the in-plane $H_\parallel$ and the c-axis $H_\perp$ magnetic fields [left inset in Fig. 2(b)]. This allows us to precisely change the density of the JVs and PVs.

When the devices shown in Figs. 1 and 2 operate, vortices are driven by an external current having *two* harmonics, $I_{\rm drive}(\nu_1, \nu_2, \varphi) = I_0[\cos(2\pi\nu_1 t) + \cos(2\pi\nu_2 t + \varphi)]$, with frequencies ν_1, ν_2, and a relative phase φ. The parameters ν_2/ν_1, and ϕ can be used as *two* independent *control knobs* to easily tune the net vortex drift (the output of these devices). Note that a two-harmonics ac current provides a much more controllable way of manipulating vortex motion than, say, a dc current which, if weak enough, produces no vortex motion. A current having two harmonics was generated by a programmable function generator with a current-voltage converter.

Our experimental setup allows us to test the two different classes of nonlinear devices (shown in Figs. 1 and 2) by changing *either* (i) the applied magnetic field [Figs. 1(a) and 2(a)], (ii) the relative phase φ of the two harmonics of the driving current [Fig. 1(b), inset in Fig. 2(b)], *or* (iii) the ratio ν_2/ν_1 of the two driving frequencies [Fig. 2(b)].

When applying an ac current $I_{\rm drive}(\nu_1, \nu_2, \varphi)$ having *two* harmonics, an average dc voltage was observed for both types of vortex devices (Figs. 1 and 2) for frequencies ν_1 and ν_2 taking certain commensurate values (e.g., $\nu_2 = 0.5\nu_1$, $\nu_2 = 1.5\nu_1$, $\nu_2 = 2\nu_1$). In contrast to spatially-asymmetric vortex devices [7–14], the rectification observed here is zero if only *one*-harmonic input current is applied, e.g., when $\nu_1 = \nu_2$ [Fig. 2(b)].

Vortices moving on a spatially-symmetric potential.—Our device shown in Fig. 1, with a nanofabricated array of holes, can rectify the motion of PVs when driven by a two-harmonic current $I_{\rm drive}(\nu_1, \nu_2, \varphi)$. A set of representative data is shown in Fig. 1(a) and 1(b). Choosing the frequency ratio $\nu_2 = 2\nu_1$ and the relative phase $\varphi = 0$, we investigate [Fig. 1(a)] how the rectified dc voltage $V_{\rm dc}$ depends on the out-of-plane magnetic field $H_\perp$. At the matching fields $H_n^{\rm match}$, we observed clear maxima in the rectified voltage $V_{\rm dc}(H)$. This increase of rectification at the matching fields is related to the enhancement of vortex pinning which results in more nonlinear VI curves. The measurements [inset in Fig. 1(a)] of the dc voltage-current curves confirm this.

When intervortex interactions are comparable with pinning interactions, the VI nonlinearity is strongest. The spatial scale responsible for intervortex interactions is $\lambda_{\rm ab}(T) = \lambda_{\rm ab}(T=0)/(1-T^2/T_c^2)^{1/2}$, while scales responsible for pinning interactions near the matching fields are $a_0/\sqrt{n}$. A simple estimate, $\lambda_{\rm ab}(T_n) \approx a_0/\sqrt{n}$, defines the temperatures T_n when the nonlinearity at the nth matching is dominant. Using the standard value $\lambda_{\rm ab}(T=0) = 200$ nm, we obtain that the strongest VI nonlinearity occurs at the 1st matching field when $T \approx T_1 \approx 86$ K, while at $T \approx T_2 \approx 84$ K the strongest nonlinearity shifts to the second matching field, in perfect agreement with our experiments [compare the $T = 86.3$ and 84.8 K curves in Fig. 1(a)].

Even though varying $H_\perp$ and/or I_0 partly allow us to tune the dc output, our main goal now is to show how to manipulate the vortex motion by *only* modifying the *time*-dependence of the driving current $I_{\rm drive}(\nu_1, \nu_2, \varphi)$ since, e.g., $H_\perp$ and I_0 can be naturally fixed by external conditions. To demonstrate an unprecedented level of controllability of our devices, we present here [Fig. 1(b)] the dependence of the dc voltage $V_{\rm dc}$ ($\propto$ the drift vortex velocity) on the relative phase shift φ of the two-current harmonics. The measured cosine-type dependence of $V_{\rm dc}(\varphi)$ allows us to precisely *tune* the output of the vortex device to any desirable value $V_{\rm dc}$ between $V_{\rm dc}(\varphi = \pi)$, which is negative, and $V_{\rm dc}(\varphi = 0)$, which is positive. In particular, the current inversion (which for other systems [3–15] can require a peculiar hard-to-realize condition on either $H_\perp$, I_0, or frequency) can be achieved here by varying φ.

Another remarkable feature of the obtained output characteristic $V_{\rm dc}(\varphi)$ is its smooth and predictable dependence on the control parameter φ, which cannot be usually achieved (e.g., Ref. [24]) in the regime where the net drift changes its direction. To simulate the experimentally-obtained results, we use standard equations of overdamped dynamics (see., e.g., Ref. [3,5,6]): $\eta\mathbf{v}_i = \sum_j \mathbf{f}_{vv}(\mathbf{r}_i - \mathbf{r}_j) + \sum_k \mathbf{f}_{\rm pv}(\mathbf{r}_i - \mathbf{r}_k^{(p)}) + \mathbf{f}_L$ with viscosity coefficient η, 2D vortex velocities $\mathbf{v}_i$, and positions $\mathbf{r}_i$. This equation describes the balance between viscous forces $\eta\mathbf{v}_i$, intervortex interactions $\mathbf{f}_{\rm vv}$, interactions $\mathbf{f}_{\rm pv}$ with pinning centers located in $\mathbf{r}_k^{(p)}$, and driving Lorentz force $\mathbf{f}_L$ controlled by the driving current $I_{\rm drive} \propto |\mathbf{f}_L|$. We use parabolic-potential pinning traps with a radius $r^{(p)}$, and a logarithmic intervortex potential, which is appropriate for the thin superconducting slabs used in our experiments. We normalize the time by a relaxation time proportional to the viscosity, all forces by the characteristic intervortex force f_0, and all distances by the London penetration depth $\lambda_{\rm ab} = 200$ nm. We obtain excellent agreement between simulations and experiments, as presented, e.g., in Fig. 1(b).

Motion control of in-plane vortices.—The operation of our second class of devices (Fig. 2), rectifying motion of ac driven Josephson vortices forced by a two-harmonic input current $I_{\rm drive}(\nu_1, \nu_2, \varphi)$, is shown on Figs. 2(a) and 2(b). When changing H, which is almost parallel ($H_\perp \ll H_\parallel \approx H$) to the superconducting layers of $Bi_2Sr_2CaCu_2O_{8+\delta}$, we clearly distinguish two working regimes. At relatively low field H, its out-of-plane component $H_\perp \propto H$ is so weak that it cannot create PVs. In this regime, the nonlinearity of our device is relatively weak, producing weak rectification. Also, this rectification shows oscillations [red curve (also pointed by arrow labeled "rectified voltage") in the "JV only" regime in Fig. 2(a)] due to the matching between the length of the sample and the spatial period of the JV lattice. At higher H, PVs enter the sample producing strong pinning for JVs, which results in the abrupt drop of the voltage versus magnetic field at a fixed time-independent current [blue curve (also pointed by arrow labeled "voltage at a fixed current") in Fig. 2(a)]. This PV-JV pinning, as was predicted in Ref. [16], results in an efficient rectification

[red curve (also pointed by arrow labeled "rectified voltage") in the "JV + PV" regime in Fig. 2(a)] of the time-asymmetric two-harmonic ac-current $I_{\rm drive}(\nu_1, \nu_2 = 2\nu_1, \phi = 0)$. The rectification grows with field. As a result, the dc voltage $V_{\rm dc}$ reaches to $\sim$10% of the maximum output voltage at the highest measured $H \approx 27$ kOe. The origin of this rectification is related to the strong enhancement of the nonlinearity due to the dragging of PVs by JVs at slow velocities and the almost-decoupled vortex motion at high JV velocities. Note that the JV-PV interactions responsible for strong nonlinearity are suppressed for $T > 70$ K, limiting the working temperatures of our device.

Even if $\mathbf{H} = (H_\parallel, H_\perp)$ and I_0 are fixed, the nonlinear rectifier (Fig. 2) of JV motion has two important additional control "knobs": the relative phase φ of the two harmonics and the frequency ratio ν_2/ν_1. The dependence [right inset in Fig. 2(b)] of the rectified voltage versus phase for the JV-motion rectifier (Fig. 2) is very similar to the cosine-like dependence of the pancake vortex drift versus φ [Fig. 1(b)] in our rectifier having nanoholes (Fig. 1). This behavior is very general and could be called a "Josephson rectification effect," based on the remarkable similarity between the dependence of the rectified current versus the relative phase of the two harmonics with the usual dependence of the Josephson current versus the relative phase of the order parameters across a Josephson junction. We also measured the resonance-like behavior of $V_{\rm dc}(\nu_2)$ at a fixed ν_1 [see Fig. 2(b)]. For several ratios of ν_2/ν_1, the rectification shows either *negative* or *positive* peaks. By changing this ratio, we can easily push vortices forward or backward at will. Even though rectification shows narrow peaks, the behavior is still very predictable, which is important for potential applications. In order to show this, we simulated the dynamics of two vortex species [18,25] (PVs and JVs) by using the coupled set of differential equations: $\eta_P v_i^P = \sum_j f_{PP}(x_i^P - x_j^P) + \sum_k f_{PJ}(x_i^P - x_k^J)$ and $\eta_J v_i^J = \sum_j f_{JJ}(x_i^J - x_j^J) + \sum_k f_{PJ}(x_i^J - x_k^P) + f_L$ with an exponential repulsion of vortex rows of the same species [$f_{PP} = \pm \exp(-|x_i^P - x_j^P|)$ and $f_{JJ} = \pm f_{JJ}^0 \exp(-|x_i^J - x_k^P|/\lambda_c)$ for interactions among only PVs, and for interactions among only JVs] and an exponential attraction for rows of different species [$f_{PJ} = \mp f_{PJ}^0 \exp(-|x_i^P - x_k^J|/\lambda_{PJ})$ for JV-PV interactions]. Here, all force prefactors, f_{JJ}^0 and f_{PJ}^0, are normalized by the amplitude of the interpancake interactions, while all interaction distances, λ_c and λ_{PJ}, by the in-plane London penetration length. The Josephson and pancake vortex viscosities are η_J and η_P, while v^J, x^J (v^P, x^P) are the velocity and position of the JV (PV) rows. The normalized experimental data and simulations are in very good agreement, indicating the efficient control and tuning obtained with this nonlinear device by just changing the ratio of frequencies ν_2/ν_1.

Conclusions.—Here, we experimentally realized two different classes of nonlinear rectifiers of vortex motion driven by two-harmonic currents. In contrast to the vortex ratchets employing fixed spatial asymmetry, our rectifiers can be easily controlled by changing either the frequency ratio or the relative phase of the two harmonics of the drive. The realization of these (*high-temperature*) devices should help the growing field of superconducting vortex electronics (fluxtronics). Further extensions of these devices could allow the possibility of making novel nanoscales stepmotors driven by either periodic ac oscillations or nonequilibrium random fluctuations in magnetic fields or currents.

We acknowledge partial support from the NSA, LPS, ARO, NSF Grant Nos. EIA-0130383, JSPS-RFBR 06-02-91200, MEXT Grant-in-Aid No. 18740224 and No. 19760017, JSPS CTC and ESF AQDJJ programs, and the EPSRC via Nos. EP/D072581/1, EP/F005482/1.

[1] A. Maeda *et al.*, Phys. Rev. Lett. **94**, 077001 (2005).
[2] P. Hänggi *et al.*, Ann. Phys. (Leipzig) **14**, 51 (2005).
[3] J. F. Wambaugh *et al.*, Phys. Rev. Lett. **83**, 5106 (1999).
[4] C.-S. Lee *et al.*, Nature (London) **400**, 337 (1999).
[5] C. J. Olson *et al.*, Phys. Rev. Lett. **87**, 177002 (2001).
[6] B. Y. Zhu *et al.*, Phys. Rev. Lett. **92**, 180602 (2004).
[7] W. K. Kwok *et al.*, Physica C (Amsterdam) **382**, 137 (2002).
[8] J. E. Villegas *et al.*, Science **302**, 1188 (2003).
[9] J. Van de Vondel *et al.*, Phys. Rev. Lett. **94**, 057003 (2005).
[10] Y. Togawa *et al.*, Phys. Rev. Lett. **95**, 087002 (2005).
[11] J. B. Majer *et al.*, Phys. Rev. Lett. **90**, 056802 (2003).
[12] D. E. Shalom and H. Pastoriza, Phys. Rev. Lett. **94**, 177001 (2005).
[13] M. Beck *et al.*, Phys. Rev. Lett. **95**, 090603 (2005).
[14] C. C. de Souza Silva *et al.*, Nature (London) **440**, 651 (2006).
[15] F. Nori, Nature Phys. **2**, 227 (2006).
[16] S. Savel'ev and F. Nori, Nat. Mater. **1**, 179 (2002).
[17] A. Tonomura, Nat. Mater. **5**, 257 (2006).
[18] D. Cole *et al.*, Nat. Mater. **5**, 305 (2006).
[19] A. V. Ustinov *et al.*, Phys. Rev. Lett. **93**, 087001 (2004).
[20] S. Savel'ev *et al.*, Phys. Rev. E **70**, 066109 (2004); Europhys. Lett. **67**, 179 (2004); Eur. Phys. J. B **40**, 403 (2004).
[21] S. Savel'ev *et al.*, Phys. Rev. B **64**, 094521 (2001).
[22] T. Mochiku *et al.*, Physica C (Amsterdam) **282–287**, 475 (1997).
[23] S. Ooi *et al.*, Phys. Rev. Lett. **89**, 247002 (2002).
[24] J. L. Mateos, Phys. Rev. Lett. **84**, 258 (2000).
[25] S. Savel'ev *et al.*, Phys. Rev. Lett. **92**, 160602 (2004); **91**, 010601 (2003); Phys. Rev. E **70**, 061107 (2004); **71**, 011107 (2005); Chaos **15**, 026112 (2005). See also animation at http://dml.riken.jp/fluxtronics/NL-rectifier.swf.